Journal of ELECTRONIC MATERIALS, Vol. 45, No. 3, 2016
DOI: 10.1007/s11664-015-4070-4

Effect of Carbon Nanotubes on Thermoelectric Properties in $Zn_{0.98}Al_{0.02}O$

CHRISTIAN DREßLER,[1,3,4] ROMY LÖHNERT,[1] JESUS GONZALEZ-JULIAN,[2] OLIVIER GUILLON,[2] JÖRG TÖPFER,[1] and STEFFEN TEICHERT[1]

1.—Department SciTec, Ernst-Abbe-University of Applied Sciences Jena, Carl Zeiss Promenade 2, 07745 Jena, Germany. 2.—Institute of Energy and Climate Research: IEK-1 Materials Synthesis and Processing, Forschungszentrum Jülich GmbH, Jülich, Germany. 3.—e-mail: christian.dressler@fh-jena.de. 4.—e-mail: christian872@gmail.com

Thermoelectric oxides can provide the advantage of high-temperature stability in oxygen-containing atmospheres. It is known that the incorporation of multiwalled carbon nanotubes (mw-CNT) can change the thermoelectric as well as the structural properties of oxides. Here, we report the influence of mw-CNT on the thermoelectric properties of Al-doped ZnO (AZO). The preparation of the mw-CNT-added AZO was done using an ultrasonic mixing of the starting materials followed by a spark plasma sintering process under vacuum. The Seebeck coefficient S, thermal conductivity λ and electrical conductivity σ were determined in the temperature range between 300 K and 900 K. It was observed that the thermal conductivity is significantly reduced by the incorporation of the mw-CNT. At the same time, the electrical conductivity is increased by a factor of 21 from 8700 S/m to 190,000 S/m. The Power factor $PF = S^2\sigma$ indicates that the addition of mw-CNT improves the thermoelectric properties of Al doped ZnO in comparison to the reference sample prepared with same process but without mw-CNT.

Key words: Al doped ZnO, SPS, thermoelectric materials, carbon nanotubes

INTRODUCTION

Thermoelectric generators (TEG) are capable of converting heat directly into electrical energy. The energy conversion efficiency of thermoelectric materials depends on the material properties. It can be described by the dimensionless figure-of-merit (ZT):

$$ZT = \frac{S^2 \cdot \sigma}{\lambda} T \quad (1)$$

where S is the Seebeck coefficient, σ the electrical conductivity, λ the thermal conductivity and T the absolute temperature. It is obvious that the Seebeck coefficient and electrical conductivity need to be large and the thermal conductivity must be small to allow good thermoelectric properties. Typically, semiconductor materials such as Sb_2Te_3 (p-type) or Bi_2Te_3 (n-type) show good thermoelectric properties: Snyder et al.[1] reported a ZT value of about 1 for Sb_2Te_3 and Bi_2Te_3 at 373 K. Nevertheless, these materials show a limited stability at high temperatures in ambient conditions containing oxygen. In contrast, ceramic oxide materials have advantages, such as high chemical and temperature stability, long-term reliability and low production costs.

A series of interesting p-type ceramics such as $Bi_2Sr_2Co_2O_y$ or $Ca_3Co_4O_9$ with ZT values of about 0.4 have already been reported.[2,3] In comparison, n-type ceramics usually do not reach such high ZT values. However, zinc oxide is a promising n-type ceramic with a high Seebeck coefficient (300–400 μV/K from room temperature to 1273 K)[4,5] but it also shows low electrical and high thermal conductivity. It has been reported that the substitution of Zn by Al in ZnO improves the ZT. However, the

(Received June 1, 2015; accepted September 18, 2015; published online October 5, 2015)

literature also shows a large variation of the thermoelectric properties for the Al-doped ZnO (AZO).[4–10] For example a ZT value of 0.3 was obtained after conventional sintering at 1673 K in air.[4,5] Hot-pressed samples show a significantly lower ZT of about 0.02–0.035 at 1223 K,[6,7] whereas spark plasma sintered samples vary from 0.25 (973 K)[8] to 0.08 (673 K).[9] Al-doped nanostructured ZnO is one of the best n-type thermoelectric oxides reported to date with a ZT value of 0.44 at 1000 K.[10]

In the case of ZnO, the limitation of the ZT values are mostly related to the rather high thermal conductivity which is originated by the wurtzite crystal structure of ZnO.[11,12] One approach to enhance thermoelectric properties, particularly λ, is nanostructuring or the implementation of nanoinclusions.[13–15] This leads to an increase of phonon scattering at the grain boundaries, hence a reduction of λ. For the modification of thermoelectric materials on the nanoscale, carbon nanotubes (CNT) have recently been used. It was shown that CNT have a good thermoelectric performance which strongly depends on the type of CNT.[16–21] For multiwalled carbon nanotubes (mw-CNT), Kim et al.[21] reported an exceptionally high λ (3000 W/mK) and a Seebeck-coefficient of 80 μV/K at room temperature. For bulk mw-CNT samples, Yang et al.[22] reported a significantly lower thermal conductivity of 15 W/mK than the individual CNT. In conjunction with semiconductors[13,14] and ceramics,[23–25] CNT influence the thermoelectric[23] and structural properties.[26–30] It was shown that CNT have a significant influence on the sintering and grain growth behavior of ceramics.[27,31,32] Low contents of CNT (<2 vol.%) enhances the densification process by a better initial packing, whereas the grain growth is inhibited by Zener pinning effect.[33] Similar effects have been observed by other authors, i.e. Inam et al.[27] reported a significant grain growth inhibition on alumina pellets by addition of 5 wt.% mw-CNT. On the other hand, an increase of electrical conductivity of the compacts by the addition of CNTs is not expected to substantially affect the sintering behavior due to the high electrical conductivity of the graphite system in comparison with the sample.[33]

In this work, we investigate the influence of the incorporation of mw-CNT into Al-doped ZnO. We sintered a composite consisting of Al-doped ZnO with an addition of 0.1 wt.% mw-CNT by field-assisted sintering technique/spark plasma sintering (FAST/SPS).[34] The thermal and electrical properties of the pressed sample with mw-CNT were compared with those of pure AZO.

EXPERIMENTAL

For the fabrication of $Zn_{0.98}Al_{0.02}O$ (AZO) powders, a commercially available ZnO (Norzinco; BET <1 μm) was mixed in stoichiometric ratio with nanosized 6 wt.% Al-doped ZnO (Sigma Aldrich, BET <100 nm). Afterwards, 0.1 wt.% mw-CNT (Sigma Aldrich) with a diameter of 6 nm to 9 nm and a length of 10 nm up to 5 μm were added. To get a homogeneous, well-dispersed mixture of AZO and mw-CNT, the powders were mixed dispersed in a solvent (2-propanol) for 15 min in an ultrasonic bath, then mixed by an ultrasonic finger for 4 min and stirred again for 15 min in an ultrasonic bath. Finally, the solvent was evaporated slowly on a heating plate at 348 K. The dried powders were mechanically milled in an agate ball mill for 30 min.

For the densification of the $Zn_{0.98}Al_{0.02}O$/CNT composite, a spark plasma sintering (SPS) apparatus was used. One gram of homogeneous mix of AZO and mw-CNT was filled in a graphite die of 10 mm inner diameter and prepressed at 50 MPa. Besides, a graphite foil was located between the powders and the graphite die and punches in order to ensure the thermal and the electrical contacts. Temperature was controlled by a thermocouple placed in a drilled hole in the middle of the graphite die and located 10 mm from the powder. The graphite die was surrounded by a carbon felt in order to reduce the heating loss. The sintering was done under vacuum (40 Pa) to avoid combustion of the mw-CNT. The composites were densified at a heating rate of 373 K/min from room temperature to 873 K and 323 K/min from 873 K to 1173 K. Isothermal holding time at 1173 K was maintained for 10 min. A constant pressure of 50 MPa was applied during the whole sintering process. The diameter of the samples after sintering was 10 mm.

The crystalline phase analysis was done using a x-ray diffractometer (D8 Discover, Bruker). The microstructure of the $Zn_{0.98}Al_{0.02}O$/CNT composites was analyzed by a field emission scanning electron microscope (Ultra 55, Zeiss). An image analysis using the intercept procedure (ASTM E112) with a correction factor of 1.56 was performed to determine the grain size. The thermal conductivity λ was calculated by $\lambda = \alpha \cdot c_p \cdot D$. The thermal diffusivity α (LFA 1000, Linseis) was measured from 298 K to 873 K in He atmosphere. For a better laser coupling into the samples, a carbon coating was required. The heat capacity c_p (STA PT1600, Linseis) was measured from 298 K to 873 K in Ar atmosphere and the density D was determined by the Archimedes method. The Seebeck coefficient S and electrical conductivity σ of cylindrical-shaped samples were measured with a commercial setup (LSR-3, Linseis) in He atmosphere. The measuring temperature was changed from room temperature to 873 K.

RESULTS AND DISCUSSION

All SPS sintered composites showed a high density of $94 \pm 2\%$. For pure AZO, the theoretical density of ZnO (5.61 g/cm^3) was used. The calculation of theoretical density of $Zn_{0.98}Al_{0.02}O$ with 0.1 wt.% mw-CNT (5.606 g/cm^3) was also done using the theoretical density of the CNT (2.0 g/cm^3).

All reflexes in the x-ray diffraction pattern of the $Zn_{0.98}Al_{0.02}O$/CNT composite (Fig. 1) could be attributed to ZnO. No indication of the occurrence of the spinel phase $ZnAl_2O_4$[5,7,8] could be found within the XRD detection limits. The doping of Al into the ZnO lattice is indicated by a small shift of the XRD patterns to larger 2θ values compared to the reference of pure ZnO.[11]

The comparison of the grain structure and grain size of both samples reveals no major influence of the mw-CNT on the microstructure (Fig. 2). The typical grain size was in the range of 0.5–1.0 μm for both sample types. Figure 3 shows the thermal and electrical properties of pure $Zn_{0.98}Al_{0.02}O$ and the mw-CNT-added composite as a function of the temperature. The electrical conductivity σ (Fig. 3a) increases by adding mw-CNT. The σ of pure AZO was approximately 8700 S/m in the whole temperature range. In the case of 0.1 wt.% mw-CNT-containing AZO, σ reaches a maximum of 192,000 S/m at 373 K. All samples indicate a metallic-like behavior, i.e. σ decreases with temperature. The considerable increase in σ is probably due to the well-distributed mw-CNT along the grain boundaries of AZO. This network of mw-CNT forms a new electrical pathway through the $Zn_{0.98}Al_{0.02}O$/CNT composite which leads to a local change of σ at the grain boundaries. The mw-CNT may offer shortcuts between the AZO grains as was shown by Cho et al. in a nanotube–copper matrix composite[36]

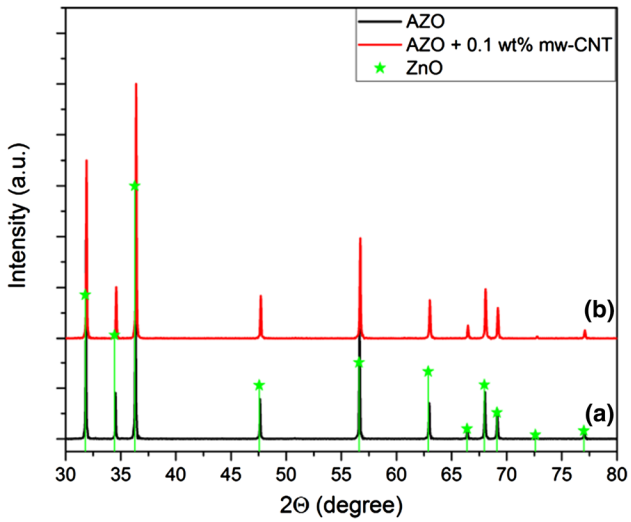

Fig. 1. X-ray diffraction pattern of SPS sintered $Zn_{0.98}Al_{0.02}O$/CNT composites with (a) 0.0 wt.%, (b) 0.1 wt.% and reference phase ZnO (PDF-Nr. 01-070-8070).[35]

Figure 3b shows the Seebeck-coefficient (S) of the $Zn_{0.98}Al_{0.02}O$/CNT composite. The negative values indicate n-type semiconducting behavior. It is obvious that with increasing temperature the absolute value of the Seebeck coefficient also increases. The S of pure AZO ranged from -80 μV/K at room temperature (RT) up to -145 μV/K at 873 K, which corresponds well to previously published data.[4] The addition of 0.1 wt.% mw-CNT leads to a significant decrease in S to -40 μV/K at room temperature (RT).

The thermal conductivity λ of the $Zn_{0.98}Al_{0.02}O$/CNT composite decreases with increasing temperature, as shown in Fig. 3c. As expected, λ decreased with 0.1 wt.% mw-CNT. At room temperature, λ was reduced by about 16%, from 31.2 W/mK (pure AZO) to 26 W/mK. A similar effect has already been reported[25] and interpreted in terms of an additional phonon scattering due to the mw-CNT. The level of the reduction depends on the thermal properties of the carbon nanotubes used.[20,37] With increasing temperature, the thermal conductivity of pure and mw-CNT-added AZO converged.

In Fig. 3d, the power-factor PF of the $Zn_{0.98}Al_{0.02}O$/CNT is shown. The PF determines the performance of thermoelectric power generators and was calculated by the formula $PF = S^2 \cdot \sigma$. The

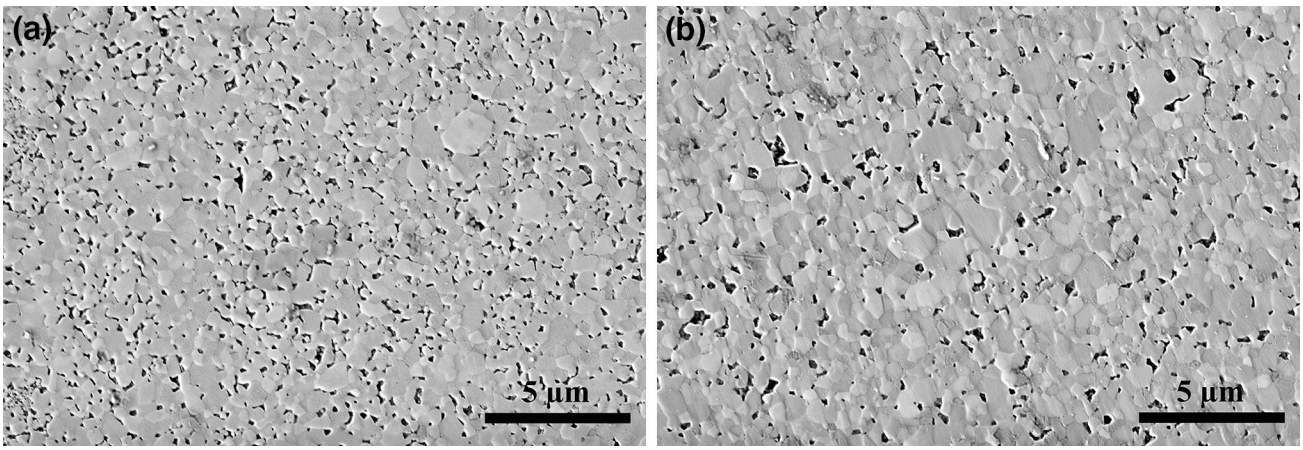

Fig. 2. SEM micrographs of (a) pure and (b) 0.1 wt.% mw-CNT added $Zn_{0.98}Al_{0.02}O$.

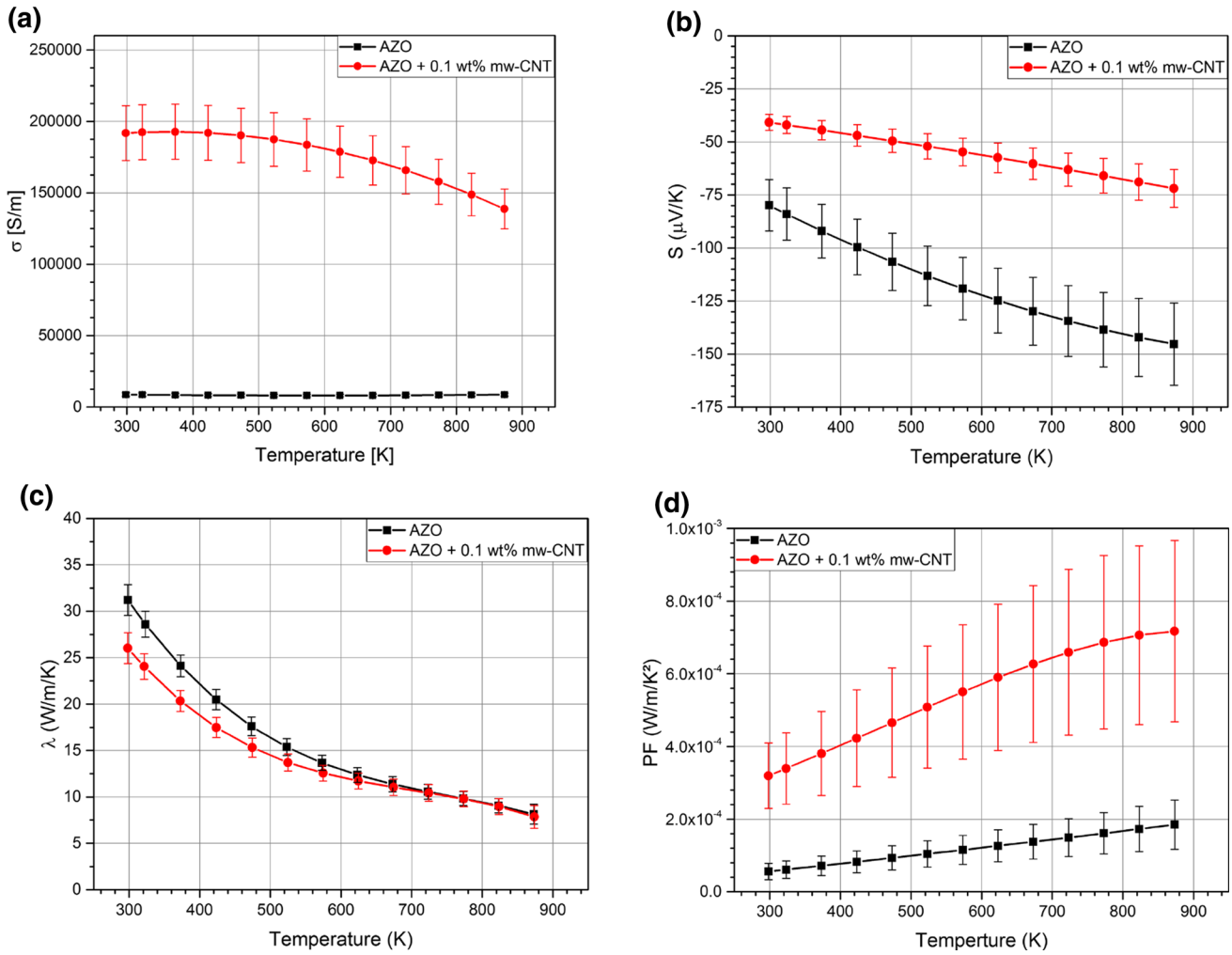

Fig. 3. The thermoelectric properties of the $Zn_{0.98}Al_{0.02}O$/CNT composite versus temperature: (a) electrical conductivity (σ) (b) Seebeck coefficient (S) (c) thermal conductivity (λ) and (d) power-factor (PF).

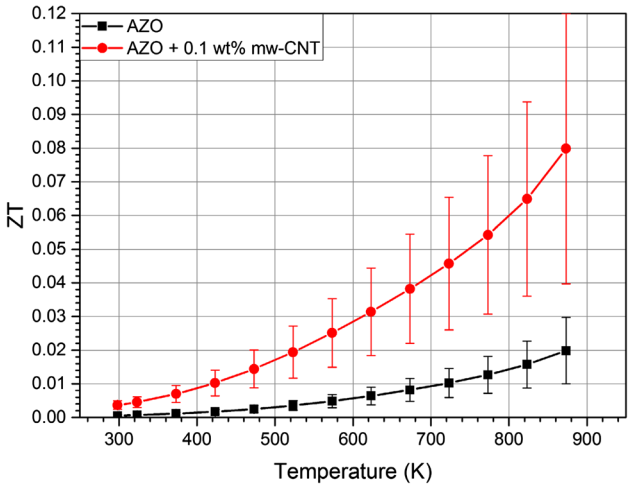

Fig. 4. Dimensionless figure of merit (ZT) of the $Zn_{0.98}Al_{0.02}O$/CNT composite.

maximum value of 7.2×10^{-4} W/mK^2, is obtained for a content of 0.1 wt.% mw-CNT at 873 K.

The results for the $Zn_{0.98}Al_{0.02}O$ with mw-CNT show an improvement of the electrical and thermal conductivity at the same time. These changes overcompensate the reduction of the Seebeck coefficient resulting in an improved ZT of the composite with 0.1 wt.% mw-CNT. The ZT ranged from 0.02 (873 K) for pure AZO to 0.08 (873 K) for 0.1 wt.% mw-CNT-containing AZO, which is an increase of ZT by a factor of 4 (Fig. 4). The obtained ZT values are less than the known values from the literature. Possible causes are due to a short holding time (10 min) or the sintering temperature of 1173 K.

SUMMARY

In summary, we prepared a composite consisting of Al-doped ZnO and mw-CNT with SPS. The ther-

moelectric properties of pure AZO and mw-CNT-added AZO have been characterized in detail. It has been shown that the incorporation of mw-CNT increases the electrical conductivity and decreases the thermal conductivity. This is achieved by enhancing the phonon scattering at the grain boundaries caused by the incorporation of mw-CNT. It was revealed that an amount of 0.1 wt.% mw-CNT, in comparison to pure AZO, increases the electrical conductivity by a factor of 21 over the entire temperature range. The thermal conductivity is reduced by the factor of 1.2 at room temperature. In general, the results show the enhancement of ZT by the factor of 4 from 0.02 to 0.08 at 873 K.

ACKNOWLEDGEMENT

The work was financially supported within the Project "NOXTHERMO" by the Federal Ministry of Education and Research Germany (03FH003I2).

REFERENCES

1. G.J. Snyder and E.S. Toberer, *Nat. Mater.* 7, 105 (2008).
2. R. Funahashi and M. Shikano, *Appl. Phys. Lett.* 81, 1459 (2002).
3. M.A. Madre, F.M. Costa, N.M. Ferreira, A. Sotelo, M.A. Torres, G. Constantinescu, and J.C. Diez, *J. Eur. Ceram. Soc.* 33, 1747 (2013).
4. T. Tsubota, M. Ohtak, K. Eguchi, and H. Arai, *J. Mater. Chem.* 7, 85 (1997).
5. M. Ohtaki, T. Tsubota, K. Eguchi, and H. Arai, *J. Appl. Phys.* 79, 1816 (1996).
6. K.F. Cai, E. Müller, C. Drašar, and A. Mrotzek, *Mater. Sci. Eng., B* 104, 45 (2003).
7. H. Cheng, X.J. Xu, H.H. Hng, and J. Ma, *Ceram. Int.* 35, 3067 (2009).
8. M. Søndergaard, E.D. Bøjesen, K.A. Borup, S. Christensen, M. Christensen, and B.B. Iversen, *Acta Mater.* 61, 3314 (2013).
9. N. Ma, J.-F. Li, B.P. Zhang, Y.H. Lin, L.R. Ren, and G.F. Chen, *J. Phys. Chem. Solids* 71, 1344 (2010).
10. P. Jood, R.J. Mehta, Y. Zhang, G. Peleckis, X. Wang, R.W. Siegel, and G. Ramanath, *Nano Lett.* 11, 4337 (2011).
11. F. Maldonado and A. Stashans, *J. Phys. Chem. Solids* 71, 784 (2010).
12. U. Özgür, Y.I. Alivov, C. Liu, A. Teke, M.A. Reshchikov, S. Doğan, V. Avrutin, S.-J. Cho, and H. Morkoç, *J. Appl. Phys.* 98, 041301 (2005).
13. K.T. Kim, S.Y. Choi, E.H. Shin, K.S. Moon, H.Y. Koo, G.-G. Lee, and G.H. Ha, *Carbon* 52, 541 (2013).
14. D.-H. Park, M.-Y. Kim, and T.-S. Oh, *Curr. Appl. Phys.* 11, 41 (2011).
15. S.V. Faleev and F. Leonard, *Phys. Rev. B* 77, 214304 (2008).
16. I. Kunadian, R. Andrews, M. Pinar Mengüç, and D. Qian, *Carbon* 47, 589 (2009).
17. G. Sumanasekera, B. Pradhan, H. Romero, K. Adu, and P. Eklund, *Phys. Rev. Lett.* 89, 166801 (2002).
18. J. Hone, I. Ellwood, M. Muno, A. Mizel, M.L. Cohen, and A. Zettl, *Phys. Rev. Lett.* 80, 1042 (1998).
19. R.H. Baughman, A.A. Zakhidov, and W.A. de Heer, *Science* 297, 787 (2002).
20. M.J. Biercuk, M.C. Llaguno, M. Radosavljevic, J.K. Hyun, and A.T. Johnson, *Appl. Phys. Lett.* 80, 2767 (2002).
21. P. Kim, L. Shi, A. Majumdar, and P. McEuen, *Phys. Rev. Lett.* 87, 215502 (2001).
22. D.J. Yang, Q. Zhang, G. Chen, S.F. Yoon, J. Ahn, S.G. Wang, and J.Q. Li, *Phys. Rev. B* 66, 165440 (2002).
23. G.-D. Zhan, J.D. Kuntz, A.K. Mukherjee, P. Zhu, and K. Koumoto, *Scr. Mater.* 54, 77 (2006).
24. G.-D. Zhan, J.D. Kuntz, J.E. Garay, and A.K. Mukherjee, *Appl. Phys. Lett.* 83, 1228 (2003).
25. G.-D. Zhan and A.K. Mukherjee, *Int. J. Appl. Ceram. Technol.* 1, 161 (2004).
26. B. Milsom, G. Viola, Z. Gao, F. Inam, T. Peijs, and M.J. Reece, *J. Eur. Ceram. Soc.* 16, 4149 (2012).
27. F. Inam, H. Yan, T. Peijs, and M.J. Reece, *Compos. Sci. Technol.* 70, 947 (2010).
28. J. Fan, D. Zhao, M. Wu, Z. Xu, and J. Song, *J. Am. Ceram. Soc.* 89, 750 (2006).
29. M. Michálek, M. Kašiarová, M. Michálková, and D. Galusek, *J. Eur. Ceram. Soc.* 34, 3329 (2014).
30. J. Cho, F. Inam, M.J. Reece, Z. Chlup, I. Dlouhy, M.S.P. Shaffer, and A.R. Boccaccini, *J. Mater. Sci.* 46, 4770 (2011).
31. S. Sarkar and P.K. Das, *Mater. Sci. Eng., A* 531, 61 (2012).
32. S.C. Zhang, W.G. Fahrenholtz, G.E. Hilmas, and E.J. Yadlowsky, *J. Eur. Ceram. Soc.* 30, 1373 (2010).
33. A.M. Zahedi, J. Gonzalez-Julian, M. Mazaheri, J. Javadpour, H.R. Rezaie, and O. Guillon, *J. Eur. Ceram. Soc.* 35, 4241 (2015).
34. O. Guillon, J. Gonzalez-Julian, B. Dargatz, T. Kessel, G. Schierning, J. Räthel, and M. Herrmann, *Adv. Eng. Mater.* 16, 830 (2014).
35. K. Yoshio, A. Onodera, H. Satoh, N. Sakagami, and H. Yamashita, *Ferroelectrics* 264, 133 (2001).
36. S. Cho, K. Kikuchi, and A. Kawasaki, *Acta Mater.* 60, 726 (2012).
37. V. Vretenár, V. Skákalová, Ľ. Kubičár, and V. Boháč, in *Conference Proceedings*, 67–75 (2003).